Received: 13 December 2016 | Revised: 15 May 2018 | Accepted: 20 June 2018

DOI: 10.1002/hbm.24303

WILEY

RESEARCH ARTICLE

Clinical subcategorization of minimally conscious state according to resting functional connectivity

Charlène Aubinet[1] | Stephen Karl Larroque[1] | Lizette Heine[2] | Charlotte Martial[1] | Steve Majerus[3] | Steven Laureys[1] | Carol Di Perri[1,4]

[1]Coma Science Group, GIGA Research Center and Neurology Department, University and University Hospital of Liège, Liège, Belgium

[2]Auditory Cognition and Psychoacoustics Team – Lyon Neuroscience Research Center (UCBL, CNRS UMR5292, Inserm U1028), Lyon, France

[3]Psychology and Neuroscience of Cognition Research Unit, University of Liege, Belgium

[4]Centre for Clinical Brain Sciences UK Dementia Research Institute, Centre for Dementia Prevention, University of Edinburgh, Edinburgh, United Kingdom

Correspondence
Charlène Aubinet, CHU de Liège, GIGA research (B34, +1), Avenue de l'Hôpital 1, 4000 Liège, Belgium.
Email: caubinet@uliege.be

Funding information
The University and University Hospital of Liège, French Speaking Community Concerted Research Action, Grant/Award Number: ARC 12-17/01; Belgian National Funds for Scientific Research (FRS-FNRS); Human Brain Project, Grant/Award Number: EU-H2020-fetflagship-hbp-sga1-ga720270; Luminous project, Grant/Award Number: EU-H2020-fetopen-ga686764; James S. McDonnell Foundation; Mind Science Foundation; IAP research network P7/06 of the Belgian Government (Belgian Science Policy); European Commission; Public Utility Foundation "Université Européenne du Travail"; "Fondazione Europea di Ricerca Biomedica"; Fundação Bial, Belgian National *Plan Cancer* (139)

Abstract

Patients in minimally conscious state (MCS) have been subcategorized in MCS *plus* and MCS *minus*, based on command-following, intelligible verbalization or intentional communication. We here aimed to better characterize the functional neuroanatomy of MCS based on this clinical subcategorization by means of resting state functional magnetic resonance imaging (fMRI). Resting state fMRI was acquired in 292 MCS patients and a seed-based analysis was conducted on a convenience sample of 10 MCS *plus* patients, 9 MCS *minus* patients and 35 healthy subjects. We investigated the left and right frontoparietal networks (FPN), auditory network, default mode network (DMN), thalamocortical connectivity and DMN between-network anticorrelations. We also employed an analysis based on regions of interest (ROI) to examine interhemispheric connectivity and investigated intergroup differences in gray/white matter volume by means of voxel-based morphometry. We found a higher connectivity in MCS *plus* as compared to MCS *minus* in the left FPN, specifically between the left dorso-lateral prefrontal cortex and left temporo-occipital fusiform cortex. No differences between patient groups were observed in the auditory network, right FPN, DMN, thalamocortical and interhemispheric connectivity, between-network anticorrelations and gray/white matter volume. Our preliminary group-level results suggest that the clinical subcategorization of MCS may involve functional connectivity differences in a language-related executive control network. MCS *plus* and *minus* patients are seemingly not differentiated by networks associated to auditory processing, perception of surroundings and internal awareness/self-mentation, nor by interhemispheric integration and structural brain damage.

KEYWORDS

auditory network, default mode network, frontoparietal network, functional connectivity, language, MCS *minus* and *plus*, resting state fMRI, structural imaging

1 | INTRODUCTION

Disorders of consciousness are characterized by prolonged impaired awareness following a severe brain damage (Laureys, Perrin, et al., 2004). Patients in coma are neither awake nor aware, but this condition usually lasts no longer than four weeks. When patients awaken but show no signs of awareness of self and surroundings, they are said to have unresponsive wakefulness syndrome (i.e., vegetative state) (Laureys et al., 2010). When patients recover minimal yet definite behavioral evidence of self or environmental awareness, they are said to be in a minimally conscious state (MCS) (Giacino et al., 2002). The MCS diagnosis has been further subcategorized into MCS *minus* and MCS *plus* (Bruno et al., 2012; Bruno, Vanhaudenhuyse, Thibaut, Moonen, & Laureys, 2011). The most frequent signs of consciousness in MCS *minus* patients are visual fixation and pursuit, automatic motor reactions (e.g., scratching, pulling the bed sheet) and localization to

noxious stimulation (Wannez, Gosseries, et al., 2017), whereas MCS *plus* patients can, in addition, follow simple commands, intelligibly verbalize or intentionally communicate (Bruno et al., 2011).

Several neuroimaging studies have suggested a key role of networks encompassing associative cortices on the midline (internal awareness network or default mode network [DMN]) and on the convexity (external awareness network or frontoparietal network [FPN]) for the emergence of consciousness (Laureys, Owen, & Schiff, 2004; Vanhaudenhuyse et al., 2011). In particular, studies using resting-state functional magnetic resonance imaging (fMRI), a noninvasive technique investigating the spontaneous temporal coherence in blood-oxygen-level dependent (BOLD) fluctuations (Raichle et al., 2001), have shown that DMN functional connectivity increases along with the level of consciousness, from coma to healthy consciousness (through unresponsive wakefulness syndrome, MCS and emerging from MCS) (Demertzi et al., 2015; Di Perri et al., 2016; Vanhaudenhuyse et al., 2011). In a similar manner, functional connectivity of the FPN has shown to be impaired in disorders of consciousness and this impairment is more severe in the unresponsive wakefulness syndrome than in MCS (Crone et al., 2014). Furthermore, the FPN, classically considered as an executive control network (Reineberg & Banich, 2016; Smith et al., 2009), has been subdivided into the right FPN, known to be involved in somesthesic processing and nociceptive perception (Laird et al., 2011; Smith et al., 2009), and the left FPN, considered to be related to executive language processing (Geranmayeh, Leech, & Wise, 2016; Laird et al., 2011; Smith et al., 2009) and to act as a "semantic control system" by interacting with a left perisylvian network and with the DMN (Xu, Lin, Han, He, & Bi, 2016).

Recent studies have further highlighted the role of DMN between-network anticorrelations (i.e., anticorrelations between the DMN and FPN) in the recovery of consciousness (Di Perri et al., 2016). The strength of DMN (between-network) anticorrelations correlates positively with the level of consciousness ranging from unresponsive wakefulness syndrome to healthy consciousness. In particular, only patients who emerged from the MCS and healthy control subjects (HCS) showed these DMN between-network anticorrelations. Patients in altered states of consciousness had atypical positive correlations between the two networks, suggesting that anticorrelations characterize the level of consciousness involved in functional communication and object use. These findings imply that DMN anticorrelations may play an important role in internetwork information integration during consciousness by allowing for alternation between extrospectively-oriented and introspectively-oriented modes of function (Fransson, 2005); this aspect has also been considered to be indicative of subjectivity or conscious awareness (Demertzi, Vanhaudenhuyse, et al., 2013). Similarly, thalamocortical connections were shown to play a crucial role in patients' behavioral profile and complex information integration sustaining conscious awareness, by means of both structural and neurophysiological studies (Estraneo et al., 2016; Kim, Hwang, Kang, Kim, & Choi, 2012; Zheng, Reggente, Lutkenhoff, Owen, & Monti, 2017).

While several studies have, to date, focused on characterizing the levels of consciousness and prognostic factors in patients with disorders of consciousness (Demertzi et al., 2015; Di Perri et al., 2016; Laureys, Bodart, & Gosseries, 2014; Stender et al., 2014), their residual cognitive functions still remain poorly investigated. It has been shown that patient's own name stimulation activated associative areas in unresponsive patients who subsequently evolved to MCS (Di et al., 2007). By contrasting connectivity responses to intelligible and unintelligible speech in two MCS patients, Schiff and colleagues (Schiff et al., 2005) showed a residual cortical activity related to language processing in these patients despite their inability to follow simple commands. Similarly, using fMRI during a silent picture-naming task, five MCS patients demonstrated at least a partial preservation of the language network (Rodriguez Moreno, Schiff, Giacino, Kalmar, & Hirsch, 2010). More recently, connectivity responses to diverse auditory stimulations (words vs. pseudo-words or semantically-related vs. semantically-non related words) were analyzed in MCS and unresponsive patients (Nigri et al., 2016). Their results suggested a residual automatic lexical processing in the linguistic networks of both patient groups. Evidence of context-dependent higher-order auditory processing in severely brain injured patients have also been provided by means of positron emission tomography (PET) (Laureys, Perrin, et al., 2004) and event-related potential paradigms (Beukema et al., 2016; Kotchoubey et al., 2005).

Using fluorodeoxyglucose PET in resting state, Bruno et al. (2012) found a metabolic impairment in a bilateral subcortical (thalamus and caudate) and cortical (fronto-temporo-parietal) network in traumatic and nontraumatic patients in MCS. Nevertheless, as compared to MCS *minus*, patients in MCS *plus* showed preserved cerebral metabolism in left-sided cortical areas, including language-related areas such as Broca's (1861) and Wernicke's areas. Although the influence of motor skills, memory and volition on command-following abilities has to be taken into account, such findings further suggest a critical role of language functions in the MCS subcategorization. In other words, MCS *minus* patients may present reduced residual language abilities as compared to MCS *plus* patients. It is further important to stress here that MCS *minus* patients have multiple domain impairment as compared to aphasic patients and hence cannot be simply equated to aphasic patients.

We here aimed to better characterize the functional neuroanatomy of MCS based on its clinical subcategorization into MCS *plus* and MCS *minus* by means of resting state fMRI. Given that previous studies in conscious aphasic patients showed an impairment of connectivity between structures in the left FPN (Kümmerer et al., 2013; Zhu et al., 2014), we hypothesized a higher connectivity in MCS *plus* as compared to MCS *minus* in this language-related executive control network (Smith et al., 2009). We also investigated the DMN, the auditory network and right FPN—which are known to differ between different altered states of consciousness (Crone et al., 2014; Demertzi et al., 2015; Di Perri et al., 2016; Estraneo et al., 2016; Laureys et al., 2000; Vanhaudenhuyse et al., 2011; Zheng et al., 2017)—to test whether the clinical subcategorization of MCS might reflect differences in networks involved in internal awareness or self-related mentation, auditory processing and perception of surroundings, respectively (Laird et al., 2011). We further aimed at investigating whether the subcategories of MCS *minus* and *plus* are sustained by differences in interhemispheric connectivity in the networks of interest (Teki et al., 2013). Indeed, whether the reestablishment of left–right hemisphere connectivity plays a role in residual language abilities in MCS *plus* patients is still unclear. Given that language is left hemisphere dominant (Klingbeil, Wawrzyniak, Stockert, & Saur, 2017; McAvoy et al., 2016) and that recovery of

language in conscious aphasic patients can involve compensatory mechanisms in the contralateral right hemisphere (Artzi, Shiran, Weinstein, Myers, & Tarrasch, 2016; Heiss, Kessler, Thiel, Ghaemi, & Karbe, 1999; Teki et al., 2013), the restoration of left–right hemisphere connections might play a particular role in the transition from MCS *minus* to MCS *plus*. In addition, to control for the influence of anatomical deformations on functional connectivity changes (Demertzi et al., 2015; Di Perri et al., 2016), we investigated group differences in gray and white matter volume by means of voxel-based morphometry. In light of previous studies showing no unequivocal relationship between morphology and disorders of consciousness (Demertzi et al., 2015; Di Perri et al., 2016; Tshibanda et al., 2010) we did not expect brain morphology to be significantly different between MCS subgroups. Finally, we investigated DMN anticorrelations and thalamocortical functional connectivity, known to be different in patients with impaired consciousness as compared to conscious subjects (Di Perri et al., 2016; Estraneo et al., 2016; Kim et al., 2012; Zheng et al., 2017). In line with previous resting-state fMRI studies which did not show differences in anticorrelations between patients with various disorders of consciousness (Di Perri et al., 2016; Zhou et al., 2011), we did not expect these markers to be significantly different between the MCS subgroups.

2 | MATERIALS AND METHOD

2.1 | Participants

Patients were included in the study after being behaviorally assessed with the Coma Recovery Scale-Revised (Giacino et al., 2002; Schnakers et al., 2008; Seel et al., 2010), which allowed us to categorize the patients as being MCS *plus* or MCS *minus*. To reduce misdiagnosis, at least five repeated clinical assessments within a short time interval (e.g., one week) were conducted by a team of experienced neuropsychologists. The highest score within that time interval was retained for final diagnosis (Wannez, Heine, Thonnard, Gosseries, & Laureys, 2017). The diagnostic criteria for each clinical condition are summarized in Table S1 (Supporting Information 1). Exclusion criteria were: (a) time postinjury less than 28 days, (b) motion artifacts requiring sedation or anesthesia during scanning, (c) motion parameters greater than 3 mm in translation and/or 3° in rotation (leading to exclusion of subjects), (d) large focal brain damage (i.e., more than 2/3 of one hemisphere) as stated by a certified neuroradiologist who was blind to patients' diagnosis (i.e., behavioral profile and research imaging findings), (e) suboptimal segmentation and normalization as stated by a certified neuroradiologist, (f) left-handedness. Moreover, HCS free of psychiatric or neurological history were included in the present research.

The study was approved by the Ethics Committee of the Faculty of Medicine in the University of Liège. Written informed consent to participate in the study was obtained from the HCS and from the legal surrogates of the patients.

2.2 | Data acquisition

Resting-state fMRI: 300 T2*-weighted resting state fMRI volumes (Echo Planar Imaging sequence: 32 slices, repetition time = 2,000 ms, echo time = 30 ms, field of view = 192 × 192 mm^2, flip angle = 78°, voxel size = 3 × 3 × 3 mm^3) were acquired on a 3 T scanner (Siemens Trio Tim, Munich, Germany), in one run of 10 min and 6 s.

Structural Imaging: For anatomical reference and further volumetric anatomical analysis, a high-resolution T1-weighted image was acquired per subject (T1-weighted 3D gradient echo images using 120 slices, repetition time = 2,300 ms, echo time = 2.47 ms, voxel size = 1 × 1 × 1.2 mm^3, flip angle = 9°, field of view = 256 × 256 mm^2).

2.3 | Data preprocessing

Resting-state fMRI: Data preprocessing was performed using Statistical Parametric Mapping 8 (SPM 8; www.fil.ion.ucl.ac.uk/spm). Preprocessing steps consisted of: slice-time correction, realignment, co-registration of functional on structural data, spatial normalization with the diffeomorphic anatomical registration through an exponentiated lie algebra (DARTEL) (Ashburner, 2007; Takahashi et al., 2010) and smoothing with Gaussian isotropic kernel (8 mm of full-width-at-half-maximum). For the normalization procedure we used a study-template created with DARTEL obtained from patients and HCS (Ashburner, 2007; Di Perri et al., 2013; Peelle, Cusack, & Henson, 2012). This template was used to minimize normalization difficulty as it decreases the degree of warping necessary for patient brains in the normalization step and reduces the likelihood of misclassification and normalization errors that can occur during the voxel-based morphometry process. For BOLD noise reduction, we used the anatomical component-based noise correction method (Behzadi, Restom, Liau, & Liu, 2007) as implemented in the *CONN* functional connectivity toolbox (Whitfield-Gabrieli & Nieto-Castanon, 2012). The anatomical component-based noise correction process derives principal components from noise regions of interest and includes them as nuisance parameters within the general linear models. The influence of noise was modeled as a voxel-specific linear combination of multiple empirically estimated noise sources. Precisely, the anatomical image for each subject was segmented into white matter, gray matter and cerebrospinal fluid. White and cerebrospinal segments were eroded by one voxel to reduce partial voluming with gray matter (Chai, Castañán, Öngür, & Whitfield-Gabrieli, 2012). The eroded white matter and cerebrospinal fluid masks were used as noise regions of interest and their signals were deleted from the unsmoothed functional volumes to avoid additional risk of contaminating white matter and cerebrospinal fluid signals with gray matter signals. A temporal band-pass filter of .008–.09 Hz was applied on the time series, to restrict the analysis to low frequency fluctuations which characterize functional MRI BOLD resting state activity as classically performed in seed-correlation analysis (Fox et al., 2005; Greicius, Krasnow, Reiss, & Menon, 2003). Remaining head motion parameters (three rotation and three translation parameters, plus another six parameters representing their first-order temporal derivatives) were regressed out. Regarding motion correction we used the artifact detection toolbox (ART; http://nitrc.org/projects/artifact_detect) for artifact detection and rejection, using a composite motion measure (largest voxel movement) with a "liberal" threshold (global threshold 9.0, motion threshold 2.0, use scan-to-scan motion and global signal). With this approach, a volume was defined as an outlier (artifact) if the largest voxel movement detected was above the specified thresholds. Specifically, an image was defined

as an outlier (artifact) image if the head displacement in *x*, *y* or *z* direction was greater than 0.5 mm from the previous frame, or if the rotational displacement was greater than .02 rad from the previous frame, or if the global mean intensity in the image was greater than 3 *SD* from the mean image intensity for the entire resting scan. Outliers in the global mean signal intensity and motion were subsequently included as nuisance regressors (i.e., one regressor per outlier within the first-level general linear model). In doing so, the temporal structure of the data was not disrupted.

Structural imaging: A T1 voxel-based morphometry analysis of brain structure (VBM 8; http://dbm.neuro.uni-jena.de/vbm/) for SPM 8 (http://www.fil.ion.ucl.ac.uk/spm/) was carried out using DARTEL. T1 MRI images were segmented into gray and white matter and cerebrospinal fluid using the unified segmentation module. These segmented gray and white matter images were then used to obtain a more accurate intersubject registration model using DARTEL. This model alternates between computing a group template and warping the individual's tissue probability maps in alignment with this template and ultimately creates the individual flow field of each participant. We then normalized the images of each participant into a study template in MNI space to further aid the normalization procedure. The normalized images were visually controlled one by one to ensure that relative gray and white matter volumes were well preserved following spatial normalization. They were further overlaid on an MRI structural image to ensure that all regions would be overlapping.

2.4 | Statistical analysis

Resting-state fMRI: For measurement of fMRI resting state functional connectivity, a seed-based approach was performed using the *CONN* connectivity toolbox (Whitfield-Gabrieli & Nieto-Castanon, 2012). The seed-correlation analysis extracts fMRI BOLD time series from a region of interest (the seed) and determines the temporal correlation between this signal and the time series from all other brain voxels. Here, we investigated the left FPN, the right FPN, the auditory network and the DMN correlations, known to be involved in language-related executive control, perception of surroundings, audition and internal awareness, respectively (Demertzi, Soddu, & Laureys, 2013; Laird et al., 2011; Smith et al., 2009; Stawarczyk, Majerus, Maquet, & D'Argembeau, 2011). As suggested by reviewers of this manuscript, we further investigated DMN anticorrelations and functional thalamocortical connectivity, known to be related to internetwork information integration (Di Perri et al., 2016; Estraneo et al., 2016; Kim et al., 2012; Zheng et al., 2017).

For each of them we defined two seeds as 5 mm-radius spheres around peak coordinates of the two main nodes taken from the literature: left dorsolateral prefrontal cortex (DLPFC) and left inferior parietal lobule (IPL) were seeds for the left FPN; right DLPFC and right IPL were considered for the right FPN; auditory network seeds were left and right superior temporal gyrus (STG); medial prefrontal cortex (MPFC) and posterior cingulate cortex (PCC) were seeds for the DMN. To avoid circularity (Kriegeskorte, Simmons, Bellgowan, & Baker, 2009) and as previously described (Demertzi et al., 2015; Di Perri et al., 2016; Whitfield-Gabrieli & Nieto-Castanon, 2012), the seed coordinates were taken from the literature (Table 1). Both seeds of each network were analyzed separately.

The time series of each seed were used to estimate whole-brain correlation *r* maps which were then converted to normally distributed Fisher's *z* transformed correlation maps to allow for group-level comparisons. In the matrix we identified the positive correlations for each group (MCS *plus*, MCS *minus* and HCS) and the differences between MCS *plus* and *minus*, MCS *plus* and HCS, MCS *minus* and HCS. Anticorrelations were generated by computing the averaged time series in both DMN seeds (MPFC and PCC). The time series were then compared at the whole brain level using Pearson correlation, generating a statistical map of the average correlation coefficient for each voxel and the average signal of the seeded regions (Di Perri et al., 2016).

We further employed a ROI to ROI analysis using the same seeds as for the seed-voxel analysis, to investigate functional connections for each network between the right and left hemispheres in subject groups, as previously done (McKenna, Koo, Killiany,, & For The Alzheimer's Disease Neuroimaging Initiative, 2016). Each ROI from one side was correlated with all ROIs from the other side. Results were considered statistically significant at $p < .05$ family wise error (FWE) corrected at cluster level, with clusters made of voxels surviving a $p < .001$ (whole brain level) (Woo, Krishnan, & Wager, 2014).

Structural-MRI: We investigated patient group differences in gray and white matter volume by means of voxel-based morphometry using the gray matter and white matter segments previously obtained by the DARTEL segmentation, as previously described (Demertzi

TABLE 1 Seed coordinates and references

Networks	Seeds	Coordinates	References
Left FPN	Left DLPFC Left IPL	*x* = −43 *y* = 22 *z* = 34 *x* = −43.1 *y* = −47 *z* = 45.4	Fair et al. (2009) for DLPFC
Right FPN	Right DLPFC Right IPL	*x* = 43 *y* = 22 *z* = 34 *x* = 46.3 *y* = −47.6 *z* = 48.2	Rolls, Joliot, and Tzourio-Mazoyer (2015) for IPL
Auditory network	Left STG Right STG	*x* = −44 *y* = −6 *z* = 11 *x* = 44 *y* = −6 *z* = 11	Maudoux et al. (2012)
DMN	MPFC PCC	*x* = −1 *y* = 54 *z* = 27 *x* = 0 *y* = −52 *z* = 27	Raichle et al. (2001)
Thalamocortical	Left thalamus Right thalamus	*x* = −8 *y* = −20 *z* = 6 *x* = 8 *y* = −20 *z* = 6	Kinomura, Larsson, Gulyás, and Roland (1996); Laureys et al. (2000)

Abbreviations: DLPFC = dorso-lateral prefrontal cortex; DMN = default mode network; FPN = fronto-parietal network; IPL = inferior parietal lobule; MPFC = medial prefrontal cortex; PCC = posterior cingulate cortex; STG = superior temporal gyrus.

et al., 2015; Di Perri et al., 2016). In the matrix we identified the differences between MCS *plus* and *minus*, MCS *plus* and HCS, MCS *minus* and HCS. Results were considered significant at $p < .05$ FDR corrected at voxel level.

3 | RESULTS

3.1 | Patients

Between October 2009 and June 2016, 292 brain-damaged patients subsequently diagnosed as MCS were admitted into the University Hospital of Liège. Following the exclusion criteria (Flowchart 1), the analysis focused on a convenience sample of 19 right handed MCS patients: 9 MCS *minus* (2 women; aged 37 ± 14 years) and 10 MCS *plus* (2 women; aged 39 ± 12 years) patients (Table 2). Age and time postinjury did not differ between groups (Mann–Whitney *U* test: $p = 0.66$ and $p = 0.97$, respectively), neither did gender and etiology (binomial test: respectively $p = 0.91$ and $p = 0.25$ for TBI versus non-TBI, that is, cerebrovascular accident, anoxia and epilepsy). Thirty-five HCS were also recruited; again age and gender did not differ between groups (respectively Mann–Whitney *U* test: $p = 0.21$ and binomial test: $p = 0.36$–24 women, aged 41 ± 15 years).

3.2 | Resting-state fMRI

Table 3 describes the cerebral areas that are functionally connected to the investigated seeds, respectively, in HCS, MCS *plus*

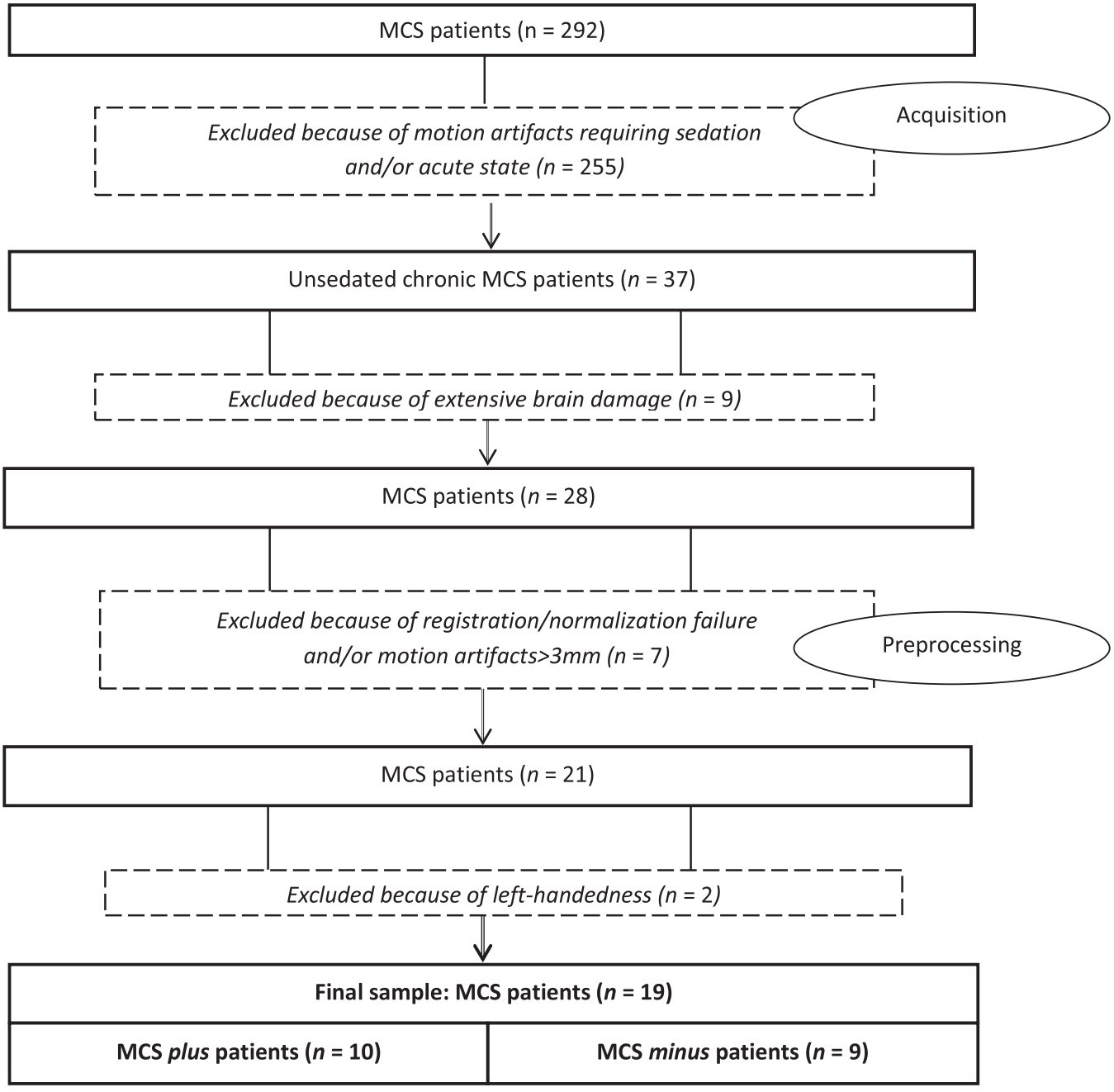

FLOWCHART 1 Patient selection based on exclusion criteria

TABLE 2 Demographic and clinical data of MCS patients

Patient	Age	Sex	Etiology	Months since onset	CRS-R best total score	Auditory functions	Visual functions	Motor functions	Oro-motor functions	Communication	Arousal	Final diagnosis
1	66	M	CVA	1,5	12	2	3	5	2	0	2	MCS-
2	27	M	TBI	12	9	1	3	2	2	0	2	MCS-
3	19	F	TBI	26	10	1	3	2	2	0	2	MCS-
4	37	M	CVA	60	10	1	3	3	2	0	2	MCS-
5	30	M	TBI—Anoxia	14	9	0	1	5	2	0	1	MCS-
6	28	M	TBI—Anoxia	3	7	1	3	2	1	0	2	MCS-
7	43	M	Anoxia	21	8	2	3	1	2	0	2	MCS-
8	45	F	TBI	8	8	2	3	2	1	0	2	MCS-
9	38	M	Anoxia	9	9	1	4	1	1	0	2	MCS-
10	34	F	TBI	96	12	3	3	2	2	0	2	MCS+
11	29	M	TBI	8	11	3	3	3	2	1	2	MCS+
12	50	M	TBI	8	13	3	4	2	2	0	2	MCS+
13	51	M	Epilepsy	2	14	3	5	2	3	1	2	MCS+
14	54	M	TBI	1,5	12	3	3	4	3	0	2	MCS+
15	29	M	TBI	1,5	9	3	4	5	2	1	2	MCS+
16	57	M	Anoxia	15	7	3	0	2	2	0	2	MCS+
17	30	F	TBI	90	8	3	0	2	2	0	2	MCS+
18	34	M	TBI	44	8	3	0	2	2	0	2	MCS+
19	23	M	TBI	22	10	3	3	3	3	0	2	MCS+

Multiple Coma Recovery Scale-Revised (CRS-R) assessments were performed. The best total score and best subscale scores among all assessments were retained.
Abbreviations: CVA = cerebrovascular accident; F = female; M = male; MCS = minimally conscious state; TBI = traumatic brain injury.

patients and MCS *minus* patients. Table 4 describes the cerebral areas showing significant between-group differences for each seed.

3.2.1 | Left frontoparietal network

In HCS, the left DLPFC and left IPL were functionally connected to the lateral frontal cortex (superior, middle and inferior frontal gyrus—more on the

TABLE 3 Network connectivity in MCS *minus* patients, MCS *plus* patients and HCS

	Left FPN	Right FPN	AN	DMN
MCS *minus*	(Figure 1a, upper row)	(Figure 2, upper row)	(Figure 3, upper row)	(Figure 4, upper row)
	Bilateral lateral frontal cortex Precuneus Left supramarginal gyrus Left angular gyrus Presupplementary motor area	Right lateral frontal cortex Precuneus Right supramarginal gyrus Right angular gyrus Supplementary motor area	Insulae Sensorimotor cortex	Anterior cingulate/ mesio-prefrontal cortex Posterior cingulate cortex/ precuneus Temporo-parietal junctions Superior frontal gyrus Angular gyrus
MCS *plus*	(Figure 1a, middle row)	(Figure 2, middle row)	(Figure 3, middle row)	(Figure 4, middle row)
	Left lateral frontal cortex Left inferior temporal cortex Left superior temporal gyrus Supramarginal gyrus Angular gyrus Precuneus Mesial frontal cortex Supplementary motor area	Right lateral frontal cortex Precuneus Right supramarginal gyrus Right angular gyrus Supplementary motor area	Insulae Sensorimotor cortex	Anterior cingulate/ mesio-prefrontal cortex Posterior cingulate cortex/ precuneus Temporo-parietal junctions Superior frontal gyrus Angular gyrus
HCS	(Figure 1a, bottom row)	(Figure 2, bottom row)	(Figure 3, bottom row)	(Figure 4, bottom row)
	Lateral frontal cortex Bilateral lateral inferior temporal cortex Precuneus Supramarginal gyrus Angular gyrus Insula Supplementary motor area	Lateral frontal cortex Lateral temporal cortex Mesial frontal cortex Precuneus Supramarginal gyrus Angular gyrus	Insulae Superior temporal gyri Sensorimotor cortex Supplementary motor cortex Supramarginal gyri	Anterior cingulate/ mesio-prefrontal cortex Posterior cingulate cortex/ precuneus Temporo-parietal junctions Angular gyri Mesial temporal cortex Superior lateral temporal cortex

Abbreviations: AN = auditory network; DMN = default mode network; FPN = fronto-parietal network; HCS = healthy control subjects; MCS = minimally conscious state.

TABLE 4 Cerebral areas showing significant between-group differences in functional connectivity

MCS *plus* > MCS *minus*	Left FPN Left temporo-occipital fusiform cortex (Figure)	Right FPN /	AN /	DMN /
HCS > MCS *plus*	Right middle frontal gyrus Right temporal pole Right angular gyrus Lateral middle/inferior frontal gyri	Left middle frontal gyrus Inferior parietal cortex Left angular gyrus Mesio-frontal cortex	Insula Sensorimotor cortex Mesio-frontal cortex	Mesial prefrontal cortex Precuneus Temporal poles
HCS > MCS *minus*	Left inferior temporal gyrus Inferior parietal cortex Right superior temporal gyrus Right angular gyrus Right middle/inferior frontal gyri	Left angular gyrus Mesio-frontal cortex	Insula Sensorimotor cortex Mesio-frontal cortex	Mesial prefrontal cortex Precuneus Temporal poles Left angular gyrus

Abbreviations: AN = auditory network; DMN = default mode network; FPN = frontoparietal network; HCS = healthy control subjects; MCS = minimally conscious state.

left side), bilateral lateral inferior temporal cortex, precuneus, supramarginal and angular gyrus (mainly on the left side), insulae, supplementary and presupplementary motor area (Figure 1a, bottom row). In MCS *plus* the left DLPFC and IPL were functionally connected to the left lateral frontal cortex, left inferior temporal cortex, left superior temporal gyrus and angular/supramarginal gyrus, the precuneus, the mesial frontal cortex and the supplementary motor area mainly on the left side (Figure 1a, middle row). In MCS *minus* the left DLPFC and IPL appeared functionally connected to the lateral frontal cortex bilaterally, to the left supramarginal/angular gyrus and to some extent to the precuneus and presupplementary motor area (Figure 1a, upper row).

MCS *plus* (as compared to MCS *minus*) showed higher connectivity between the left DLPFC and left temporo-occipital fusiform cortex (Figure c for single subject data).

HCS showed increased connectivity compared to MCS *plus* between the left DLPC and right middle frontal gyrus and between left IPL, right angular gyrus and lateral middle/inferior frontal gyri (Supporting Information Figure S1, bottom row). HCS showed increased connectivity than MCS *minus* between left DLPFC and left inferior temporal gyrus and the inferior parietal cortex, as well as between left IPL and right superior temporal gyrus, right angular gyrus and right middle/inferior frontal gyrus (Supporting Information Figure S1, upper row).

3.2.2 | Right frontoparietal network

In HCS, the right DLPFC and IPL were functionally connected to the lateral frontal cortex (more extensively on the right side), to the lateral temporal cortex, the precuneus, mesial frontal cortex and supramarginal/angular gyrus (more extensively on the right side) (Figure 2, bottom row). In MCS *plus* and *minus* the right DLPFC and IPL were functionally connected to the right supramarginal/angular gyrus, right lateral frontal cortex and supplementary motor area (Figure 2, upper and middle row). MCS *plus* showed to some extent connectivity also in the mesial right frontal cortex and precuneus (Figure 2, middle row). No differences were detected between MCS *plus* and *minus*.

HCS showed higher connectivity than MCS *plus* in left middle frontal gyrus, inferior parietal cortex, left angular gyrus (Supporting Information Figure S2, bottom row). HCS showed higher connectivity than MCS *minus* in the left angular gyrus and mesial frontal cortex (Supporting Information Figure S2, upper row).

3.2.3 | Auditory network

In HCS the right and left superior temporal gyri (STG) were functionally connected to the insulae, superior temporal gyri, sensorimotor cortex, supplementary motor cortex, supramarginal gyri (Figure 3, bottom row). In MCS *plus* and *minus* right and left STG were functionally connected to the insulae, and to a certain extent sensorimotor cortex (Figure 3, upper and middle row). No significant differences were observed between MCS *plus* and *minus*.

HCS showed higher connectivity than MCS *plus* and *minus* in the insulae, sensorimotor cortex and mesial frontal cortex (Supporting Information Figure S3).

3.2.4 | Default mode network

In HCS the MPFC and the PCC seeds showed connectivity with the precuneus, temporo-parietal junctions, angular gyri, mesial temporal cortex and superior lateral temporal cortex (Figure 4, bottom row). In MCS *plus* and *minus* the MPFC appeared functionally connected to the superior frontal gyrus and the PCC with the precuneus, temporo-parietal junctions and angular gyrus (in MCS *plus*; Figure 4, upper and middle row). No differences between MCS *plus* and *minus* were observed.

HCS showed higher connectivity than MCS *plus* in MPFC/mesial prefrontal cortex, PCC/precuneus and temporal poles (Supporting Information Figure S4, bottom row). HCS showed higher connectivity than MCS *minus* more extensively in MPFC/mesial prefrontal cortex, PCC/precuneus and temporal poles and also in the left angular gyrus (Supporting Information Figure S4, middle and upper row).

3.2.5 | Thalamocortical connectivity

In the HCS the left and right thalamus were functionally connected to the MPFC, PCC/precuneus, insulae, orbitofrontal cortices and left angular gyrus (Supporting Information Figure S8, upper row). HCS compared to MCS *minus* patients showed increased connectivity between the thalamus and the superior frontal gyrus, the cingulate cortex, precuneus and MPFC (Supporting Information Figure S8, middle row). HCS compared to MCS *plus* patients showed higher functional connectivity between the thalamus and MPFC, angular/supramarginal gyrus (Supporting Information Figure S8, bottom row).

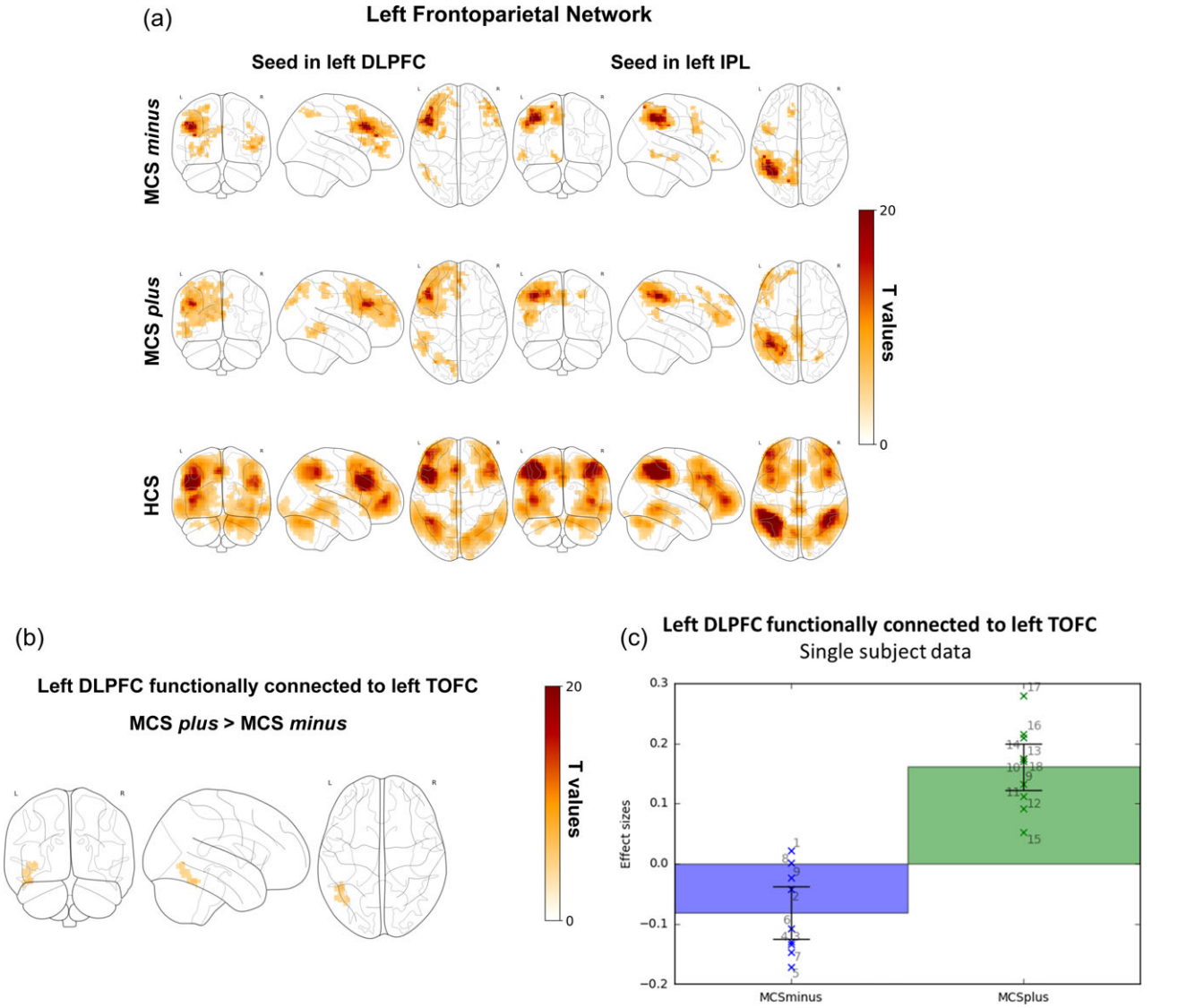

FIGURE 1 (a) Correlation between the left DLPFC (left column), left IPL (right column) and the time series from all other brain voxels in MCS *minus* (upper row), MCS *plus* (middle row) and HCS (bottom row). Statistical maps are thresholded at $p < .05$ family wise error corrected at cluster level, with clusters made of voxels surviving a $p < .001$(whole-brain level) and are rendered on the midline and lateral surfaces of a single subject's MRI template. The color bar indicates T values. This figure was displayed in neurological convention. DLPFC: Dorsolateral prefrontal cortex, IPL: Inferior parietal lobule, MCS: Minimally conscious state, HCS: Healthy control subjects. (b) Difference between MCS *minus* and *plus* according to the correlation between the left DLPFC and the time series from all other brain voxels. Statistical maps are thresholded at $p < .05$ family wise error corrected at cluster level, with clusters made of voxels surviving a $p < .001$(whole-brain level) and are rendered on the midline and lateral surfaces of a single subject's MRI template. The color bar indicates T values. This figure was displayed in neurological convention. DLPFC: Dorsolateral prefrontal cortex, TOFC: Temporo-occipital fusiform cortex, MCS: Minimally conscious state. (c) Comparison of the correlation of the voxel timeseries between the left dorsolateral prefrontal cortex (DLPFC) and the left temporo-occipital fusiform cortex (TOFC) between MCS *minus* and MCS *plus*, averaged over all significant clusters. The first bar represents mean contrast estimates with 90% confidence interval in patients in MCS (minimally conscious state) *minus* (blue); the second bar represents mean contrast estimates with 90% confidence interval in MCS *plus* patients (green). Crosses represent single subject average correlation values, with the number referring to specific subjects as shown in Table 1. Statistical maps are thresholded at $p < .05$ family wise error corrected at cluster level, with clusters made of voxels surviving a $p < .001$(whole-brain level). MCS: Minimally conscious state [Color figure can be viewed at wileyonlinelibrary.com]

3.2.6 | Interhemispheric connectivity

In the ROI to ROI connectivity analysis HCS showed higher connectivity as compared to MCS *minus* patients between right and left STG, right and left IPL and between MPFC and PCC. HCS showed higher connectivity as compared to MCS *plus* patients between right and left STG, right and left DLPFC, right and left IPL and between MPFC and PCC (Supporting Information Table S4). No differences were observed between MCS *plus* and MCS *minus*.

3.2.7 | DMN anticorrelations

In HCS compared to MCS *minus* and MCS *plus* groups anticorrelations have been observed in the lateral frontal and parietal hemispheres, insulae, supplementary/presupplementary motor regions and cuneus

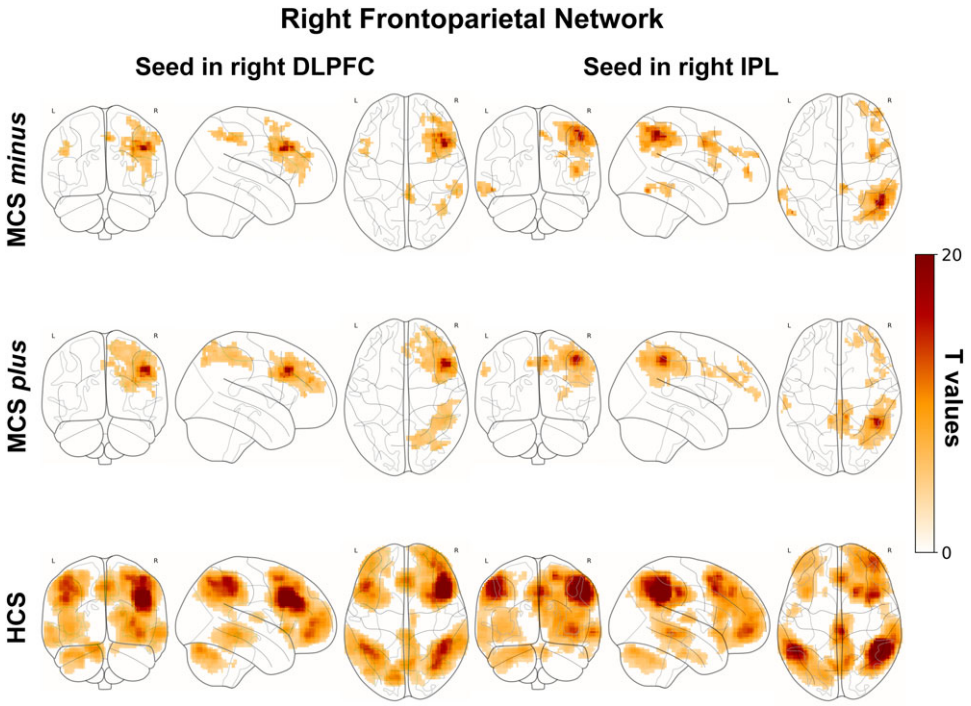

FIGURE 2 Correlation between the right DLPFC (left column), right IPL (right column) and the time series from all other brain voxels in MCS *minus* (upper row), MCS *plus* (middle row) and HCS (bottom row). Statistical maps are thresholded at $p < .05$ family wise error corrected at cluster level, with clusters made of voxels surviving a $p < .001$ (whole-brain level) and are rendered on the midline and lateral surfaces of a single subject's MRI template. The color bar indicates T values. This figure was displayed in neurological convention. DLPFC: Dorsolateral prefrontal cortex, IPL: Inferior parietal lobule, MCS: Minimally conscious state, HCS: Healthy control subjects [Color figure can be viewed at wileyonlinelibrary.com]

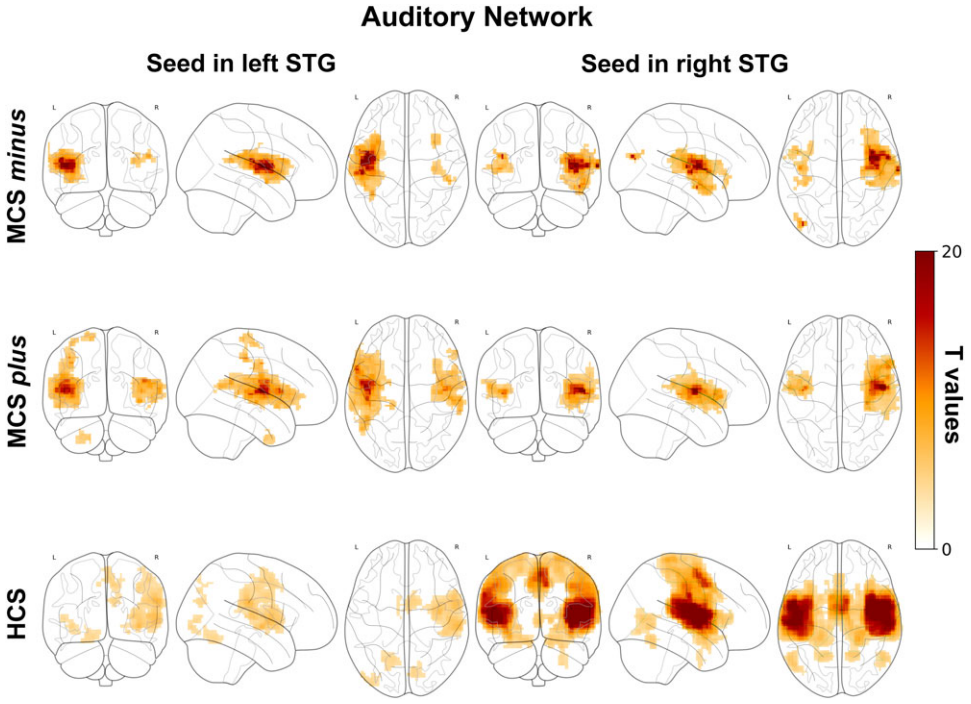

FIGURE 3 Correlation between the left STG (left column), right STG (right column) and the time series from all other brain voxels in MCS *minus* (upper row), MCS *plus* (middle row) and HCS (bottom row). Statistical maps are thresholded at $p < .05$ family wise error corrected at cluster level, with clusters made of voxels surviving a $p < .001$ (whole-brain level) and are rendered on the midline and lateral surfaces of a single subject's MRI template. The color bar indicates T values. This figure was displayed in neurological convention. STG: Superior temporal gyrus, MCS: Minimally conscious state, HCS: Healthy control subjects [Color figure can be viewed at wileyonlinelibrary.com]

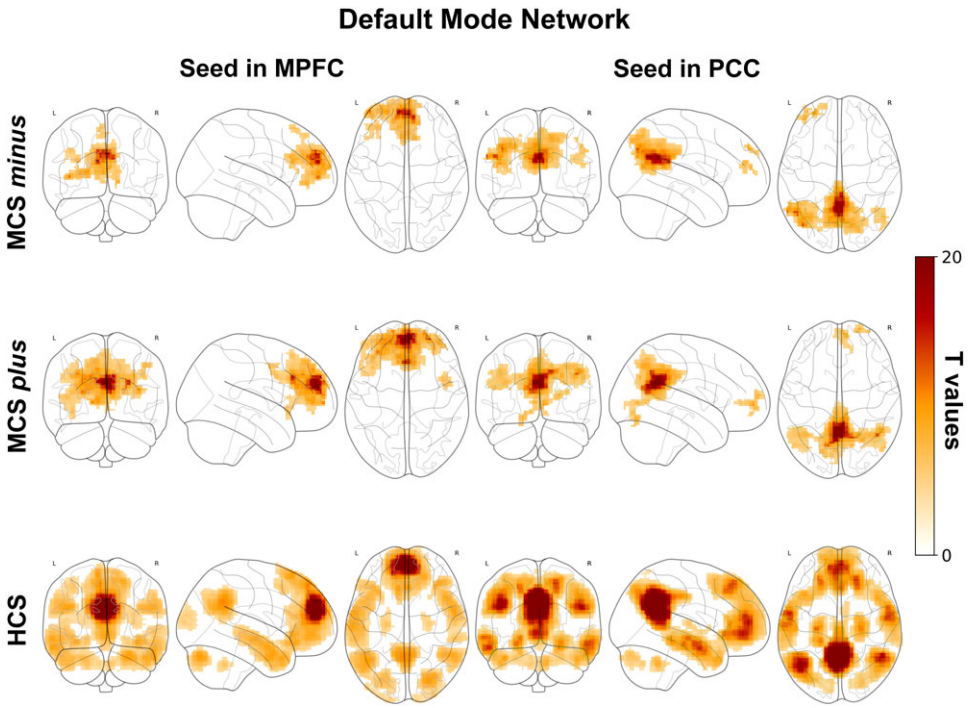

FIGURE 4 Correlation between the MPFC (left column), PCC (right column) and the time series from all other brain voxels in MCS *minus* (upper row), MCS *plus* (middle row) and HCS (bottom row). Statistical maps are thresholded at $p < .05$ family wise error corrected at cluster level, with clusters made of voxels surviving a $p < .001$ (whole-brain level) and are rendered on the midline and lateral surfaces of a single subject's MRI template. The color bar indicates T values. This figure was displayed in neurological convention. MPFC: Medial prefrontal cortex, PCC: Posterior cingulate cortex, MCS: Minimally conscious state, HCS: Healthy control subjects [Color figure can be viewed at wileyonlinelibrary.com]

(Supporting Information Figure S9). A similar pattern of anticorrelations was observed for the MCS *minus* and MCS *plus* groups.

3.3 | Structural MRI

MCS *minus* and MCS *plus* patients showed reduced gray matter volume as compared to HCS broadly involving the fronto-temporo-parietal regions and the cerebellum (Supporting Information Figure S6). Patients also showed widespread white matter decrease as compared to HCS, involving the corpus callosum, mesencephalon, occipital regions and lateral fronto-parieto-temporal regions mainly on the left hemisphere (Supporting Information Figure S7). No differences in gray and white matter were detected between MCS *plus* and MCS *minus*.

4 | DISCUSSION

In this study, we aimed to better characterize the functional neuroanatomy of MCS subcategories (Bruno et al., 2011) by means of resting-state fMRI. As expected, for all four networks, as well as for thalamocortical connectivity and between-network anticorrelations, the HCS showed significantly higher functional connectivity than MCS *minus* and MCS *plus* patients. This is in line with a large amount of literature showing impaired connectivity in patients compared to HCS in the left and right FPN, the auditory network and the DMN (Demertzi et al., 2015; Di Perri et al., 2016; Kirsch et al., 2017), thalamocortical connectivity (Estraneo et al., 2016; Zheng et al., 2017) and between-network anticorrelations (Di Perri et al., 2016). In addition we found differences between patient groups only in the left FPN, a language-related executive control network (Smith et al., 2009). Specifically, we found higher connectivity between the left DLPFC and the left temporo-occipital fusiform cortex in MCS *plus* as compared to MCS *minus* patients.

Such a difference in functional connectivity detected between patient groups corroborates previous literature associating the left FPN with language-related control (Laird et al., 2011; Smith et al., 2009) such as semantic control (Xu et al., 2016). For example, Zhu et al. (2014) showed impairment of this network in patients presenting language alterations. The authors investigated resting state fMRI and clinical evaluation of language function in poststroke aphasic patients and found reduced functional connectivity between the left FPN and the right middle frontal cortex, medial frontal cortex and right inferior frontal cortex in their patients. They also found a significant association between the degree of connectivity breakdown of the left FPN and the patients' comprehension abilities, suggesting that stroke lesions might have influenced language comprehension by altering within-network intrinsic connectivity (Zhu et al., 2014). Furthermore, reorganization of this functional network was associated to the recovery of language function, as shown through greater improvement in language function after stroke recovery (Sharp, Turkheimer, Bose, Scott, & Wise, 2010; Van Hees et al., 2014).

Furthermore, these main findings are consistent with a previous PET study (Bruno et al., 2012) showing metabolic impairment in MCS *minus* as compared to MCS *plus* patients in a fronto-temporo-parietal network involving Broca's and Wernicke's regions, left premotor, left caudate and postcentral/precentral cortices. They therefore suggest

that the proposed subcategorization of MCS based on command-following, intelligible verbalization and intentional communication (Bruno et al., 2011) is supported by differences in resting state functional connectivity in the left FPN. In particular, the alteration between the left DLPFC and the left temporo-occipital fusiform cortex (Brodmann Area 37) in MCS *minus* involves regions that have been associated with language processing and control of verbal information. The left temporo-occipital fusiform cortex has been identified as an "extended Wernicke's area" (Ardila, Bernal, & Rosselli, 2016), which is mainly dedicated to receptive language abilities. This region is also considered to link visual and semantic information (Ardila, Bernal, & Rosselli, 2015; Vigneau et al., 2006). The left temporo-occipital fusiform cortex has furthermore been shown to be involved in semantic categorization and matching of visual material (Adams & Janata, 2002; Binder et al., 1997; Damasio et al., 2001), but also in word versus nonword reading (Cohen et al., 2002; Fiez, Balota, Raichle, & Peterson, 1993). In sum, connectivity alterations in this area might signal language deficits in MCS *minus* patients, which in turn might prevent them from following commands, verbalization and intentional communication. In a future perspective, this information might be integrated into machine learning classifiers and complement clinical diagnosis at the single subject level, as required by clinical practice. Machine learning classifiers could integrate information about functional connectivity differences between MCS *plus* and MCS *minus* categories to enhance the diagnostic accuracy and sensitivity of computerized classification procedures.

As previously stated the observed differences in functional connectivity of the left FPN between both patient groups compared to HCS are in line with the literature (Kirsch et al., 2017). We here observed decreased connectivity in this language executive control network in MCS *plus* compared to MCS *minus* patients suggesting that MCS patients and HCS could be placed along a continuum, from severe left FPN dysfunction, possibly associated to severely impaired language processing in MCS *minus* patients, to preserved network connectivity in HCS, with MCS *plus* patients being situated between these two groups.

In the present study, we did not find between-patient group differences in functional connectivity of the right FPN and the auditory network, suggesting that command-following, intelligible verbalization and intentional communication capacities that distinguish the two subgroups cannot be explained by the functional status of these networks (Laird et al., 2011). Nor did we find any difference in DMN correlations, suggesting that the MCS subcategorization might not be related to internal awareness/self-related mentation known to be supported by the DMN (Demertzi et al., 2015; Vanhaudenhuyse et al., 2011). Taken together, our preliminary findings show that the clinical MCS *minus* and *plus* subcategorization involves differences in networks related to language processing, and that language residual abilities may be an important characteristic of the MCS *plus* subcategory.

The DMN is linked to cognitive processes related to internal thoughts, mind wandering and autobiographical memory (Stawarczyk et al., 2011), as well as to conscious awareness more generally (Demertzi, Soddu, et al., 2013). Some resting state fMRI studies suggest that activity of the DMN is reduced as a function of the level of impairment of consciousness, with the strongest reductions of activity observed in coma and unresponsive wakefulness syndrome (Di Perri et al., 2016; Heine et al., 2012). The above findings suggest that MCS *plus* and MCS *minus* may differ in language processing, but not in their internal thoughts or mind-wandering, despite the fact that internal thoughts might be linked to inner-speech and therefore to language processing (Alderson-Day & Fernyhough, 2015; Corballis, 2013; Jones & Fernyhough, 2007). A study in HCS showed that only 17% of resting-state experiences were language-based (Delamillieure et al., 2010), while other dominant types of mental activities were visual mental imagery (35%), somato-sensory awareness (7%), inner musical experience (6%) and mental manipulation of numbers (1%). Our results may, therefore, imply that these latter mental activities would be similarly impaired in MCS *minus* and MCS *plus* patients, and that the clinical subcategorization of MCS patients could reflect a difference in language rather than in conscious awareness. We should also note that such a dissociation between connectivity of DMN and left FPN was found in different cases of language impaired conditions, such as logopenic primary progressive aphasia (Humphreys, Hoffman, Visser, Binney, & Lambon Ralph, 2015; Lehmann et al., 2016; Whitwell et al., 2015).

The fact that we did not find differences between patient groups in interhemispheric connectivity suggests that recovery of command-following, intelligible verbalization and/or intentional communication in severely brain injured patients is not related to differences in interhemispheric connectivity. These results are in line with a recent study showing that recovery of language function relies on intact left intrahemispheric functional connectivity (Siegel et al., 2016). Further studies are needed to specify the lateralization of command-following, intelligible verbalization and intentional communication in a healthy brain, but also to better investigate possible language mechanisms in severely brain injured patients.

Our findings regarding anticorrelation patterns in patients and HCS align with previous studies reporting a rich interplay between internal and external modes of functioning which has been linked to conscious behavior (Di Perri et al., 2016; Leech, Kamourieh, Beckmann, & Sharp, 2011). Indeed, it has been shown that the degree to which DMN and FPN (internal and external awareness networks) are anticorrelated is linked to cognitive function, suggesting that stronger anticorrelations reflect a better capacity to switch between internal and external modes of attention, which sustains cognitive abilities necessary for conscious awareness (Di Perri et al., 2016; Leech et al., 2011). The lack of differences in anticorrelations between patient groups is consistent with a recent study showing no significant differences between various disorders of consciousness (Di Perri et al., 2016).

With respect to structural damages, we did not observe differences in gray and white matter volume between MCS *minus* and *plus* patients using voxel-based morphometry. This is consistent with previous studies (Demertzi et al., 2015; Di Perri et al., 2016; Tshibanda et al., 2010) and suggests that the identified differences in functional connectivity are not related to morphological differences.

These results might help reduce misdiagnosis of MCS patients and better characterize their residual abilities and cognitive potential, which in turn could help implement the most appropriate therapeutic and rehabilitative approach. For example, in behaviorally unresponsive patients who show neurophysiological or neuroimaging signs of

preserved left FPN, clinical examination of levels of consciousness should be repeated and nonverbal means of communication such as brain computer interface devices should be considered (e.g., Gibson, Owen, & Cruse, 2016). Nevertheless, our study design is not without limitations. Our sample size is limited to 19 patients. Due to this small sample and its heterogeneity, any generalizability of our results (including negative findings) should be done with extreme caution and our present study should be considered a preliminary study. Nevertheless, it should be taken into account that valid resting state functional brain images in this patient population are difficult to obtain given the patients' tendency to move in the scanner, the high probability of severe brain lesions distorting brain morphometry, as well as metal and hemosiderine artifacts, which lead to a high number of patients being excluded from the study (Flowchart 1). Another point to keep in mind is that, while the most up-to-date clinical diagnostic criteria have been applied to avoid misdiagnosis (Wannez, Heine, et al., 2017), an isolated difference in language domain between the two patient groups cannot be drawn with certainty. Lack of command-following could for example be influenced by motor impairment or arousal fluctuations. Finally, our interpretations are based on the assumption of a close correspondence between resting state networks and the networks involved in active paradigms (Smith et al., 2009), and therefore should be cautiously interpreted (e.g., auditory networks observed during rest and during active listening tasks may not necessarily be exactly the same).

5 | CONCLUSION

The proposed subcategories of MCS (Bruno et al., 2011), based on residual language-related behavioral abilities, showed a different functional neuroanatomy as detected by resting-state fMRI. Patients in MCS *minus* compared to MCS *plus* showed impaired connectivity in the left FPN, a network involved in language-related executive control. Specifically, in MCS *plus* the left DLPFC was significantly more connected to the left temporo-occipital fusiform cortex, a region involved in visuo-semantic language integration. No functional connectivity differences between patient groups were observed in the auditory network, right FPN, DMN correlations and anticorrelations, nor in thalamocortical loop, interhemispheric connectivity and gray/white matter volume. These findings suggest that the proposed clinical subcategorization of MCS patients (Bruno et al., 2011) reflects differences in residual language-related functional connectivity, and that it is seemingly not influenced by auditory processing, perception of surroundings, internal awareness/self-mentation, nor by the level of integration between both hemispheres and brain structure. These preliminary results are of clinical relevance and might help to reduce the misdiagnosis of minimally conscious patients.

ACKNOWLEDGMENTS

The study was supported by the University and University Hospital of Liège, the French Speaking Community Concerted Research Action (ARC 12-17/01), the Belgian National Funds for Scientific Research (FRS-FNRS), Human Brain Project (EU-H2020-fetflagship-hbp-sga1-ga720270), Luminous project (EU-H2020-fetopen-ga686764), the James McDonnell Foundation, Mind Science Foundation, IAP research network P7/06 of the Belgian Government (Belgian Science Policy), the European Commission, the Public Utility Foundation "Université Européenne du Travail," "Fondazione Europea di Ricerca Biomedica," the Fundação Bial, Belgian National *Plan Cancer* (139).

ORCID

Charlène Aubinet http://orcid.org/0000-0001-5095-5583
Carol Di Perri http://orcid.org/0000-0003-0284-770X

REFERENCES

Adams, R. B., & Janata, P. (2002). A comparison of neural circuits underlying auditory and visual object categorization. *NeuroImage*, *16*, 361–377.

Alderson-Day, B., & Fernyhough, C. (2015). Inner speech: Development, cognitive functions, phenomenology, and neurobiology. *Psychological Bulletin*, *141*, 931–965.

Ardila, A., Bernal, B., & Rosselli, M. (2015). Language and visual perception associations: Meta-analytic connectivity modeling of Brodmann area 37. *Behavioural Neurology*, *2015*, 1–14.

Ardila, A., Bernal, B., & Rosselli, M. (2016). How localized are language brain areas? A review of Brodmann areas involvement in oral language. *Archives of Clinical Neuropsychology*, *31*, 112–122.

Artzi, M., Shiran, S. I., Weinstein, M., Myers, V., & Tarrasch, R. (2016). Cortical reorganization following injury early in life list of abbreviation 6973953, 1–19.

Ashburner, J. (2007). A fast diffeomorphic image registration algorithm. *NeuroImage*, *38*, 95–113.

Behzadi, Y., Restom, K., Liau, J., & Liu, T. T. (2007). A component based noise correction method (CompCor) for BOLD and perfusion based fMRI. *NeuroImage*, *37*, 90–101.

Beukema, S., Gonzalez-Lara, L. E., Finoia, P., Kamau, E., Allanson, J., Chennu, S., … Cruse, D. (2016). A hierarchy of event-related potential markers of auditory processing in disorders of consciousness. *NeuroImage: Clinical*, *12*, 359–371.

Binder, J. R., Mckiernan, K. A., Parsons, M. E., Westbury, C. F., Possing, E. T., Kaufman, J. N., & Buchanan, L. (1997). Neural correlates of lexical access during visual word recognition. *Journal of Cognitive Neuroscience*, *15*, 372–393.

Broca, P. (1861). Perte de la parole, ramollissement chronique et destruction partielle du lobe antérieur gauche du cerveau. *Bulletin de la Société Anthropologique*, *2*, 235–238.

Bruno, M. A., Majerus, S., Boly, M., Vanhaudenhuyse, A., Schnakers, C., Gosseries, O., … Laureys, S. (2012). Functional neuroanatomy underlying the clinical subcategorization of minimally conscious state patients. *Journal of Neurology*, *259*, 1087–1098.

Bruno, M. A., Vanhaudenhuyse, A., Thibaut, A., Moonen, G., & Laureys, S. (2011). From unresponsive wakefulness to minimally conscious PLUS and functional locked-in syndromes: Recent advances in our understanding of disorders of consciousness. *Journal of Neurology*, *258*, 1373–1384.

Chai, X. J., Castañán, A. N., Öngür, D., & Whitfield-Gabrieli, S. (2012). Anticorrelations in resting state networks without global signal regression. *NeuroImage*, *59*, 1420–1428.

Cohen, L., Lehéricy, S., Chochon, F., Lemer, C., Rivaud, S., & Dehaene, S. (2002). Language-specific tuning of visual cortex? Functional properties of the visual word form area. *Brain*, *125*, 1054–1069.

Corballis, M. C. (2013). Wandering tales: Evolutionary origins of mental time travel and language. *Frontiers in Psychology*, *4*, 1–8.

Crone, J. S., Soddu, A., Höller, Y., Vanhaudenhuyse, A., Schurz, M., Bergmann, J., … Kronbichler, M. (2014). Altered network properties of the fronto-parietal network and the thalamus in impaired consciousness. *NeuroImage: Clinical*, *4*, 240–248. https://doi.org/10.1016/j.nicl.2013.12.005

Damasio, H., Grabowski, T. J., Tranel, D., Ponto, L. L., Hichwa, R. D., & Damasio A., R. (2001). Neural correlates of naming actions and of naming spatial relations. *NeuroImage*, *13*, 1053–1064.

Delamillieure, P., Doucet, G., Mazoyer, B., Turbelin, M. R., Delcroix, N., Mellet, E., … Joliot, M. (2010). The resting state questionnaire: An introspective questionnaire for evaluation of inner experience during the conscious resting state. *Brain Research Bulletin*, *81*, 565–573.

Demertzi, A., Antonopoulos, G., Heine, L., Voss, H. U., Crone, J. S., De Los Angeles, C., … Laureys, S. (2015). Intrinsic functional connectivity differentiates minimally conscious from unresponsive patients. *Brain*, *138*, 2619–2631.

Demertzi, A., Soddu, A., & Laureys, S. (2013). Consciousness supporting networks. *Current Opinion in Neurobiology*, *23*, 239–244.

Demertzi, A., Vanhaudenhuyse, A., Brédart, S., Heine, L., di Perri, C., & Laureys, S. (2013). Looking for the self in pathological unconsciousness. *Frontiers in Human Neuroscience*, *7*, 538.

Di, H. B., Yu, S. M., Weng, X. C., Laureys, S., Yu, D., Li, J. Q., … Chen, Y. Z. (2007). Cerebral response to patient's own name in the vegetative and minimally conscious states. *Neurology*, *68*, 895–899.

Di Perri, C., Bahri, M. A., Amico, E., Thibaut, A., Heine, L., Antonopoulos, G., … Laureys, S. (2016). Neural correlates of consciousness in patients who have emerged from a minimally conscious state: A cross-sectional multimodal imaging study. *Lancet Neurology*, *15*, 830–842.

Di Perri, C., Bastianello, S., Bartsch, A. J., Pistarini, C., Maggioni, G., Magrassi, L., … Di Salle, F. (2013). Limbic hyperconnectivity in the vegetative state. *Neurology*, *81*, 1417–1424.

Estraneo, A., Loreto, V., Guarino, I., Boemia, V., Paone, G., Moretta, P., & Trojano, L. (2016). Standard EEG in diagnostic process of prolonged disorders of consciousness. *Clinical Neurophysiology*, *127*, 2379–2385.

Fair, D. A., Cohen, A. L., Power, J. D., Dosenbach, N. U. F., Church, J. A., Miezin, F. M., … Petersen, S. E. (2009). Functional brain networks develop from a "local to distributed" organization. *PLoS Computational Biology*, *5*, 14–23.

Fiez, J. A., Balota, D. A., Raichle, M. E., & Peterson, S. E. (1993). The effects of word frequency and spelling-to-sound regularity on the functional anatomy of reading. *Society for Neuroscience – Abstracts*, *19*, 1808.

Fox, M. D., Snyder, A. Z., Vincent, J. L., Corbetta, M., Van Essen, D. C., & Raichle, M. E. (2005). The human brain is intrinsically organized into dynamic, anticorrelated functional networks. *Proceedings of the National Academy of Sciences of the United States of America*, *102*, 9673–9678.

Fransson, P. (2005). Spontaneous low-frequency BOLD signal fluctuations: An fMRI investigation of the resting-state default mode of brain function hypothesis. *Human Brain Mapping*, *26*, 15–29. doi:10.1002/hbm.20113

Geranmayeh, F., Leech, R., & Wise, R. J. S. (2016). Network dysfunction predicts speech production after left hemisphere stroke. *Neurology*, *86*, 1296–1305.

Giacino, J. T., Ashwal, S., Childs, N., Cranford, R., Jennett, B., & Katz, D. I. (2002). The minimally conscious state. *Neurology*, *58*, 349–353.

Gibson, R. M., Owen, A. M., & Cruse, D. (2016). Brain–computer interfaces for patients with disorders of consciousness. *Progress in Brain Research*, *228*, 241–291.

Greicius, M. D., Krasnow, B., Reiss, A. L., & Menon, V. (2003). Functional connectivity in the resting brain: A network analysis of the default mode hypothesis. *Proceedings of the National Academy of Sciences of the United States of America*, *100*, 253–258.

Heine, L., Soddu, A., Gómez, F., Vanhaudenhuyse, A., Tshibanda, L., Thonnard, M., … Demertzi, A. (2012). Resting state networks and consciousness: Alterations of multiple resting state network connectivity in physiological, pharmacological, and pathological consciousness states. *Frontiers in Psychology*, *3*, 1–12.

Heiss, W. D., Kessler, J., Thiel, A., Ghaemi, M., & Karbe, H. (1999). Differential capacity of left and right hemispheric areas for compensation of poststroke aphasia. *Annals of Neurology*, *45*, 430–438.

Humphreys, G. F., Hoffman, P., Visser, M., Binney, R. J., & Lambon Ralph, M. A. (2015). Establishing task- and modality-dependent dissociations between the semantic and default mode networks. *Proceedings of the National Academy of Sciences of the United States of America*, *112*, 201422760.

Jones, S. R., & Fernyhough, C. (2007). Neural correlates of inner speech and auditory verbal hallucinations: A critical review and theoretical integration. *Clinical Psychology Review*, *27*, 140–154.

Kim, S.-P., Hwang, E., Kang, J.-H., Kim, S., & Choi, J. H. (2012). Changes in the thalamocortical connectivity during anesthesia-induced transitions in consciousness. *Neuroreport*, *23*, 294–298.

Kinomura, S., Larsson, J., Gulyás, B., & Roland, P. E. (1996). Activation by attention of the human reticular formation and thalamic intralaminar nuclei. *Science*, *271*, 512–515.

Kirsch, M., Guldenmund, P., Ali Bahri, M., Demertzi, A., Baquero, K., Heine, L., … Laureys, S. (2017). Sedation of patients with disorders of consciousness during neuroimaging. *Anesthesia and Analgesia*, *124*, 588–598.

Klingbeil, J., Wawrzyniak, M., Stockert, A., & Saur, D. (2017). Resting-state functional connectivity: An emerging method for the study of language networks in poststroke aphasia. *Brain and Cognition*, pii: S0278–2626(17)30107-0.

Kotchoubey, B., Lang, S., Mezger, G., Schmalohr, D., Schneck, M., Semmler, A., … Birbaumer, N. (2005). Information processing in severe disorders of consciousness: Vegetative state and minimally conscious state. *Clinical Neurophysiology*, *116*, 2441–2453.

Kriegeskorte, N., Simmons, W. K., Bellgowan, P. S. F., & Baker, C. I. (2009). Circular analysis in systems neuroscience: The dangers of double dipping. *Nature Neuroscience*, *12*, 535–540.

Kümmerer, D., Hartwigsen, G., Kellmeyer, P., Glauche, V., Mader, I., Klöppel, S., … Saur, D. (2013). Damage to ventral and dorsal language pathways in acute aphasia. *Brain*, *136*, 619–629.

Laird, A. R., Fox, P. M., Eickhoff, S. B., Turner, J. A., Ray, K. L., McKay, D. R., … Fox, P. T. (2011). Behavioral Interpretations of Intrinsic Connectivity Networks. *Journal of Cognitive Neuroscience*, *23*, 4022–4037.

Laureys, S., Bodart, O., & Gosseries, O. (2014). The Glasgow coma scale: Time for critical reappraisal? *Lancet Neurology*, *13*, 755–757.

Laureys, S., Celesia, G. G., Cohadon, F., Lavrijsen, J., León-Carrión, J., Sannita, W. G., … Dolce, G. (2010). Unresponsive wakefulness syndrome: A new name for the vegetative state or apallic syndrome. *BMC Medicine*, *8*, 68.

Laureys, S., Faymonville, M. E., Luxen, A., Lamy, M., Franck, G., & Maquet, P. (2000). Restoration thalamocortical connect after recover from persistent veg state. *Lancet*, *355*, 1790–1791.

Laureys, S., Owen, A. M., & Schiff, N. D. (2004). Brain function in coma, vegetative state, and related disorders. *Lancet Neurology*, *3*, 537–546.

Laureys, S., Perrin, F., Faymonville, M.-E., Schnakers, C., Boly, M., Bartsch, V., … Maquet, P. (2004). Cerebral processing in the minimally conscious state. *Neurology*, *63*, 916–918.

Leech, R., Kamourieh, S., Beckmann, C. F., & Sharp, D. J. (2011). Fractionating the default mode network: Distinct contributions of the ventral and dorsal posterior cingulate cortex to cognitive control. *The Journal of Neuroscience*, *31*, 3217–3224.

Lehmann, M., Madison, C., Ghosh, P. M., Miller, Z. A., Greicius, M. D., Kramer, J. H., … Rabinovici, G. D. (2016). Loss of functional connectivity is greater outside the default mode network in nonfamilial early-onset Alzheimer's disease variants. *Neurobiology of Aging*, *36*(10), 2678–2686.

Maudoux, A., Lefebvre, P., Cabay, J. E., Demertzi, A., Vanhaudenhuyse, A., Laureys, S., & Soddu, A. (2012). Auditory resting-state network connectivity in tinnitus: A functional MRI study. *PLoS One*, *7*, 1–9.

McAvoy, M., Mitra, A., Coalson, R. S., D'Avossa, G., Keidel, J. L., Petersen, S. E., & Raichle, M. E. (2016). Unmasking language lateralization in human brain intrinsic activity. *Cerebral Cortex*, *26*, 1733–1746.

McKenna, F., Koo, B. B., Killiany, R., & For The Alzheimer's Disease Neuroimaging Initiative. (2016). Comparison of ApoE-related brain connectivity differences in early MCI and normal aging populations: An fMRI study. *Brain Imaging and Behavior*, *10*(4), 970–983.

Nigri, A., Catricalà, E., Ferraro, S., Bruzzone, M. G., D'Incerti, L., Sattin, D., … Cappa, S. F. (2016). The neural correlates of lexical processing in disorders of consciousness. *Brain Imaging and Behavior*, *11*(5), 1526–1537.

Peelle, J. E., Cusack, R., & Henson, R. N. A. (2012). Adjusting for global effects in voxel-based morphometry: Gray matter decline in normal aging. *NeuroImage*, *60*, 1503–1516.

Raichle, M. E., MacLeod, A. M., Snyder, A. Z., Powers, W. J., Gusnard, D. A., & Shulman, G. L. (2001). A default mode of brain function. *Proceedings of the National Academy of Sciences of the United States of America*, *98*, 676–682.

Reineberg, A. E., & Banich, M. T. (2016). Functional connectivity at rest is sensitive to individual differences in executive function: A network analysis. *Human Brain Mapping*, *37*, 2959–2975.

Rodriguez Moreno, D., Schiff, N. D., Giacino, J., Kalmar, K., & Hirsch, J. (2010). A network approach to assessing cognition in disorders of consciousness. *Neurology*, *75*, 1871–1878.

Rolls, E. T., Joliot, M., & Tzourio-Mazoyer, N. (2015). Implementation of a new parcellation of the orbitofrontal cortex in the automated anatomical labeling atlas. *NeuroImage*, *122*, 1–5.

Schiff, N. D., Rodriguez-Moreno, D., Kamal, A., Kim, K. H. S., Giacino, J. T., Plum, F., & Hirsch, J. (2005). fMRI reveals large-scale network activation in minimally conscious patients. *Neurology*, *64*, 514–523.

Schnakers, C., Majerus, S., Giacino, J., Vanhaudenhuyse, A., Bruno, M.-A., Boly, M., … Laureys, S. (2008). A French validation study of the coma recovery scale-revised (CRS-R). *Brain Injury*, *22*, 786–792.

Seel, R. T., Sherer, M., Whyte, J., Katz, D. I., Giacino, J. T., Rosenbaum, A. M., … Zasler, N. (2010). Assessment scales for disorders of consciousness: Evidence-based recommendations for clinical practice and research. *Archives of Physical Medicine and Rehabilitation*, *91*, 1795–1813. doi: 10.1016/j.apmr.2010.07.218

Sharp, D. J., Turkheimer, F. E., Bose, S. K., Scott, S. K., & Wise, R. J. S. (2010). Increased frontoparietal integration after stroke and cognitive recovery. *Annals of Neurology*, *68*, 753–756.

Siegel, J. S., Ramsey, L. E., Snyder, A. Z., Metcalf, N. V., Chacko, R. V., Weinberger, K., … Corbetta, M. (2016). Disruptions of network connectivity predict impairment in multiple behavioral domains after stroke. *Proceedings of the National Academy of Sciences of the United States of America*, *113*, E4367–E4376. doi:10.1073/pnas.1521083113

Smith, S. M., Fox, P. T., Miller, K. L., Glahn, D. C., Fox, P. M., Mackay, C. E., … Beckmann, C. F. (2009). Correspondence of the brain's functional architecture during activation and rest. *Proceedings of the National Academy of Sciences of the United States of America*, *106*, 13040–13045.

Stawarczyk, D., Majerus, S., Maquet, P., & D'Argembeau, A. (2011). Neural correlates of ongoing conscious experience: Both task-unrelatedness and stimulus-independence are related to default network activity. *PLoS One*, *6*, e16997.

Stender, J., Gosseries, O., Bruno, M. A., Charland-Verville, V., Vanhaudenhuyse, A., Demertzi, A., … Laureys, S. (2014). Diagnostic precision of PET imaging and functional MRI in disorders of consciousness: A clinical validation study. *Lancet*, *384*, 514–522.

Takahashi, R., Ishii, K., Miyamoto, N., Yoshikawa, T., Shimada, K., Ohkawa, S., … Yokoyama, K. (2010). Measurement of gray and white matter atrophy in dementia with lewy bodies using diffeomorphic anatomic registration through exponentiated lie algebra: A comparison with conventional voxel-based morphometry. *American Journal of Neuroradiology*, *31*, 1873–1878.

Teki, S., Barnes, G. R., Penny, W. D., Iverson, P., Woodhead, Z. V. J., Griffiths, T. D., & Leff, A. P. (2013). The right hemisphere supports but does not replace left hemisphere auditory function in patients with persisting aphasia. *Brain*, *136*, 1901–1912.

Tshibanda, L., Vanhaudenhuyse, A., Boly, M., Soddu, A., Bruno, M.-A., Moonen, G., … Noirhomme, Q. (2010). Neuroimaging after coma. *Neuroradiology*, *52*(1), 15–24.

Van Hees, S, Mcmahon, K., Angwin, A., de Zubicaray, G., Read, S., & Copland, D. A. (2014). A functional MRI study of the relationship between naming treatment outcomes and resting state functional connectivity in post-stroke aphasia. *Human Brain Mapping*, *35*, 3919–3931.

Vanhaudenhuyse, A., Demertzi, A., Schabus, M., Noirhomme, Q., Bredart, S., Boly, M., … Laureys, S. (2011). Two distinct neuronal networks mediate the awareness of environment and of self. *Journal of Cognitive Neuroscience*, *23*, 570–578.

Vigneau, M., Beaucousin, V., Hervé, P. Y., Duffau, H., Crivello, F., Houdé, O., … Tzourio-Mazoyer, N. (2006). Meta-analyzing left hemisphere language areas: Phonology, semantics, and sentence processing. *NeuroImage*, *30*, 1414–1432.

Wannez, S., Gosseries, O., Azzolini, D., Martial, C., Cassol, H., Aubinet, C., … Laureys, S. (2017). Prevalence of coma-recovery scale-revised signs of consciousness in patients in minimally conscious state. *Neuropsychological Rehabilitation*, *11*, 1–10.

Wannez, S., Heine, L., Thonnard, M., Gosseries, O., & Laureys, S. (2017). The repetition of behavioral assessments in diagnosis of disorders of consciousness. *Annals of Neurology*, *81*, 883–889. doi:10.1002/ana.24962

Whitfield-Gabrieli, S., & Nieto-Castanon, A. (2012). Conn: A functional connectivity toolbox for correlated and Anticorrelated brain networks. *Brain Connectivity*, *2*, 125–141.

Whitwell, J. L., Jones, D. T., Duffy, J. R., Strand, E. A., Machulda, M. M., Przybelski, S. A., … Josephs, K. A. (2015). Working memory and language network dysfunctions in logopenic aphasia: A task-free fMRI comparison with Alzheimer's dementia. *Neurobiology of Aging*, *36*, 1245–1252.

Woo, C. W., Krishnan, A., & Wager, T. D. (2014). Cluster-extent based thresholding in fMRI analyses: Pitfalls and recommendations. *NeuroImage*, *91*, 412–419. doi:10.1016/j.neuroimage.2013.12.058

Xu, Y., Lin, Q., Han, Z., He, Y., & Bi, Y. (2016). Intrinsic functional network architecture of human semantic processing: Modules and hubs. *NeuroImage*, *132*, 542–555. doi:10.1016/j.neuroimage.2016.03.004

Zheng, Z. S., Reggente, N., Lutkenhoff, E., Owen, A. M., & Monti, M. M. (2017). Disentangling Disorders of Consciousness : Insights From Diffusion Tensor Imaging and Machine Learning. *Human Brain Mapping*, *38*(1), 431–443.

Zhou, J., Liu, X., Song, W., Yang, Y., Zhao, Z., Ling, F., … Li, S.-J. (2011). Specific and nonspecific thalamocortical functional connectivity in normal and vegetative states. *Consciousness and Cognition*, *20*, 257–268.

Zhu, D., Chang, J., Freeman, S., Tan, Z., Xiao, J., Gao, Y., & Kong, J. (2014). Changes of functional connectivity in the left frontoparietal network following aphasic stroke. *Frontiers in Behavioral Neuroscience*, *8*, 167.

SUPPORTING INFORMATION

Additional supporting information may be found online in the Supporting Information section at the end of the article.

How to cite this article: Aubinet C, Larroque SK, Heine L, et al. Clinical subcategorization of minimally conscious state according to resting functional connectivity. *Hum Brain Mapp*. 2018;39:4519–4532. https://doi.org/10.1002/hbm.24303